

## Layered Intrusions and Regional Geology of the Nootka Sound Area, Vancouver Island, British Columbia (NTS 092E)

**K. Fecova, Department of Earth Sciences, Simon Fraser University, Burnaby, BC, [kfecova@sfu.ca](mailto:kfecova@sfu.ca)**

**D. Marshall, Department of Earth Sciences, Simon Fraser University, Burnaby, BC**

**R. Staples, Department of Earth Sciences, Simon Fraser University, Burnaby, BC**

**G. Xue, Department of Earth Sciences, Simon Fraser University, Burnaby, BC**

**T. Ullrich, Department of Ocean and Earth Sciences, University of British Columbia, Vancouver, BC**

**S. Close, Department of Earth Sciences, Simon Fraser University, Burnaby, BC**

---

Fecova, K., Marshall, D., Staples, R., Xue, G., Ullrich, T. and Close, S. (2008): Layered intrusions and regional geology of the Nootka Sound area (NTS 092E), Vancouver Island, British Columbia; *in* Geoscience BC Summary of Activities 2007, Geoscience BC, Report 2008-1, p. 35–46.

### Introduction

Layered intrusions identified in the Conuma River region of the Nootka Sound area (Marshall et al., 2006) became the subject of a detailed study during 2007. The layered intrusions consist of alternating cyclic ultramafic and mafic units of peridotite and gabbro. Fieldwork also included additional regional geological mapping of the Gold River area (NTS 092E/16). This report contains an updated preliminary geological map of the Nootka Sound region and a cross-section through the region mapped during the summers of 2004–2007. This map also shows localities with new Ar-Ar dates.

### Regional Geology

Muller et al. (1981) compiled his work and the work of others identifying the Westcoast Crystalline Complex as consisting of rocks ranging up to amphibolite metamorphic facies. It was described as a “heterogeneous assemblage of amphibolite and basic migmatite with minor metasedimentary and metavolcanic rocks of greenschist metamorphic grade.” Subsequent work (Marshall et al., 2005, 2006) revealed a lack of rocks of amphibolite grade. Instead, it confirmed the occurrence of units that are correlative with units identified in the southern portion of Vancouver Island. The exposed rocks of the Nootka Sound region appear to have a maximum regional metamorphic grade of middle greenschist facies. Contact metamorphic effects are highest near the Jurassic and Eocene intrusive

rocks, where migmatite has been observed (Muller et al., 1981).

Muller et al. (1981) designated a huge portion of the Nootka Sound region as Westcoast Crystalline Complex. Massey et al. (2005) identified the same portion of the region as Paleozoic to early Mesozoic undivided granitic rocks and lower amphibolite–kyanite grade metamorphic rocks. This work modified the earliest maps, which had dividing the region into the Mooyah Formation (Marshall et al., 2006), Mount Mark Formation (Massey, 1991; Yorath et al., 1999) and granodiorite, diorite and gabbro of the Jurassic Island Intrusive Suite. Naming polygons on the map was based on the dominance of a rock type in the area.

The geological map of the Nootka Sound area (Figure 1) compiles data from geological mapping in 2004–2007 (Close, 2006; Marshall et al., 2006). The map also uses data from Muller et al. (1981) and Massey et al. (2005), airphotos, Landsat images and maps with aeromagnetic anomalies (BC Geological Survey, 2007) to infer information on regional geology and structure for inaccessible areas.

### Layered Ultramafic and Mafic Rocks

#### Occurrence and Previous Work

The first mention regarding the occurrence of plutonic rocks of mafic nature in the Nootka Sound region comes from Muller et al. (1981). These were identified as melanosome, described as “plagioclase amphibolites with granoblastic texture and compositions of diorite, gabbro, quartz diorite and quartz gabbro” (Muller et al., 1981, p. 20), and were included as part of the Westcoast Crystalline Complex.

---

**Keywords:** *PGE mineralization, Vancouver Island, Nootka, Wrangellia, island arc, ultramafic plutonic rocks, layered intrusions*

*This publication is also available, free of charge, as colour digital files in Adobe Acrobat® PDF format from the Geoscience BC website: <http://www.geosciencebc.com/s/DataReleases.asp>.*

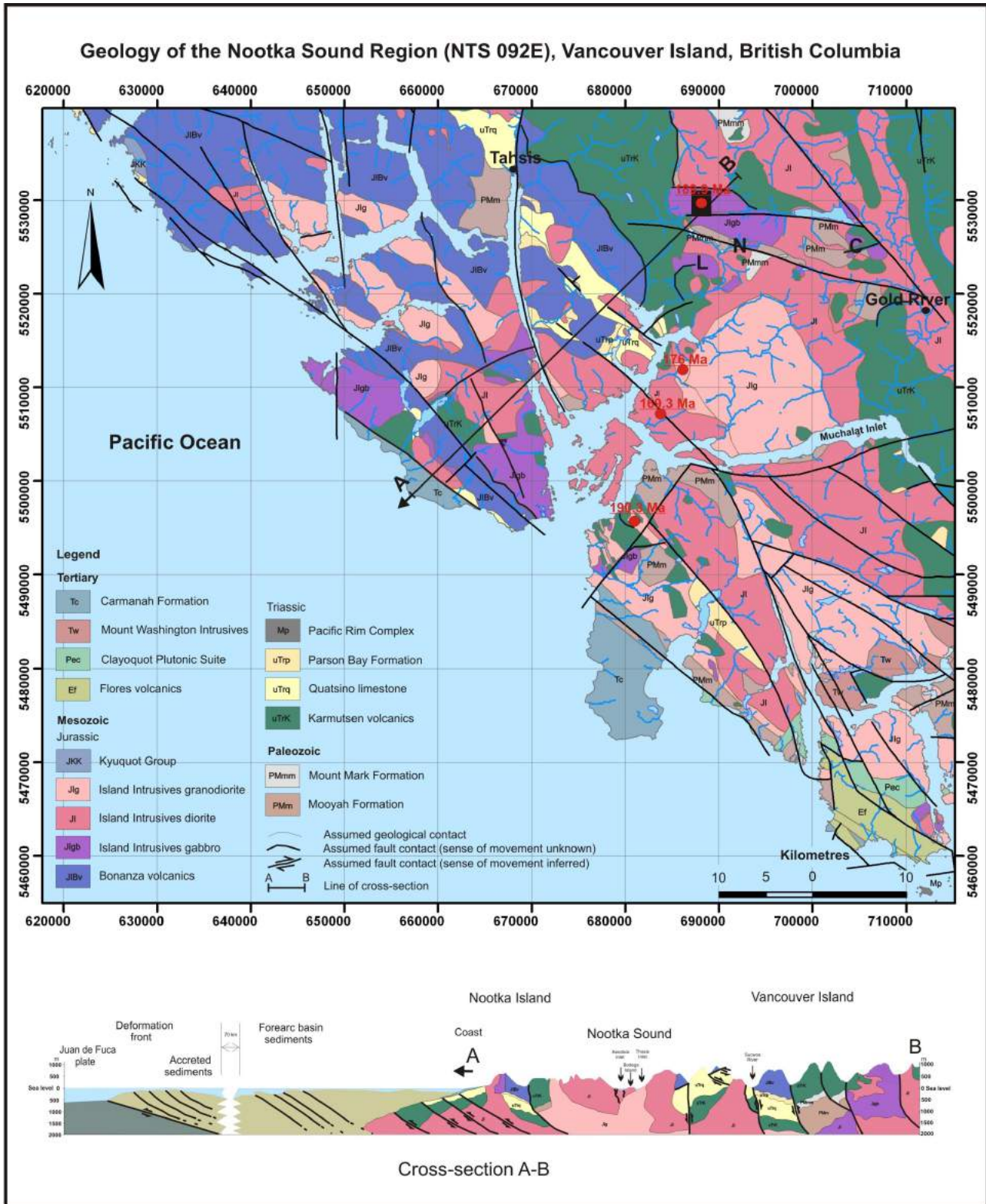


**Figure 1.** Geology of the Nootka Sound region (*modified after* Muller et al., 1981; Massey et al., 2005; Marshall et al., 2006). The map shows new Ar-Ar dates on plutonic rocks. The black rectangle depicts an area of detailed mapping that is also intersected by the cross-section A-B. Layering in intrusions in cross-section is shown by dashed parallel lines, based on the assumption that more layered intrusions outcrop in the area with similar strike and dip. Some faults were inferred from Landsat images. Abbreviations: C, Cypress Creek; L, Leigh Creek; N, Norgate Creek.

Another brief description of ultramafic and mafic rocks comes from the work of Isachsen (1987), who described the geology of the area around Meares Island. Isachsen (1987) identified outcrops within the Westcoast Crystalline Complex on Meares Island as a unit of early Jurassic or older Westcoast amphibolite. This unit is characterized by “medium to coarse grained granoblastic diorite and uralitized gabbro with granoblastic texture to fine-grained, well lined amphibolite gneiss. In places the amphibolite has a distinctive spotted texture produced by rounded, 1–3 cm diameter hornblende megacrysts in a finer grained amphibolite matrix. In some places megacrysts are aligned like beads on a string, yielding an even more striking texture, reminiscent of a cumulate” (Isachsen, 1987, p. 2049).

Isachsen (1987) also described amphibole as a replacement product after pyroxene, indicating a gabbroic parentage with 5–50% plagioclase of andesine to labradorite composition; biotite is rare and quartz is absent. The sample also shows a relatively high nickel concentration (56–211 ppm), suggesting derivation from mafic igneous rocks.

Isachsen (1987) also identified Early to Middle Jurassic gabbro and peridotite as “isolated dike like masses of uralitized gabbroic rock near the central part of Lemmens Inlet” (Isachsen, 1987, p. 2050). He described this rock type as a “medium to coarse grained unfoliated, granular gabbro-peridotite with 50% poikilitic augite with plagioclase inclusions and fibrous uralitized rims, 25% to 35% of enstatite and olivine replaced by serpentine, 10% of saussuritized bytownite, 3% of hornblende, 2% to 5% of chromite and magnetite and minor chlorite.” Sargent (1941) described similar rocks from a locality near the Bedwell River intruding the Jurassic Bedwell batholith.

The work of DeBari et al. (1999) in the Alberni area and Broken Islands area includes a description of a gabbro-peridotite unit within the Westcoast Crystalline Complex, identified by Muller et al. (1981) and Isachsen (1987). The ultramafic and mafic rocks are grouped into two pyroxene–hornblende gabbro, a pyroxenite and a sheared serpentinite of cumulate nature. Additionally, strongly foliated hornblendite, hornblende gabbro, hornblende diorite, tonalite and rare granodiorite are grouped into the diorite unit of the Westcoast Crystalline Complex. Samples yielded Jurassic ages, implying that these rock units are cogenetic with rocks of the Jurassic Island Intrusive Suite and Bonanza volcanic rocks. They also show similar whole-rock geochemistry. DeBari et al. (1999) also reported an occurrence of ultramafic cumulate near Kennedy Lake with minimal aerial extent and uncertain origin.

Larocque and Canil (2006) published preliminary results from fieldwork in the Port Renfrew area, where they found isolated bodies of ultramafic plutonic rock, which they de-

scribed as peridotite, within the Westcoast Crystalline Complex.

### Ultramafic Rocks and Local Geology of the Conuma River Area

Layered intrusions are exposed in the Conuma River area, along the C-50D logging road. The extent of the area in which they outcrop is approximately 70 m by 450 m (Figure 2).

Two types of layered intrusion are present within this area. The first type consists of 20–50 cm thick, very coarse to coarse-grained peridotite layers alternating with 20–30 cm thick, medium-grained gabbro layers (Figures 3 and 4). The second type comprises layers of very coarse grained peridotite. The layers are distinct at outcrop scale, probably due to differential weathering of certain layers. Numerous outcrops of the layered intrusions were found in the area.

The weathered surfaces of the layered intrusions are white and green for medium-grained gabbro and rusty brown for very coarse grained peridotite. At some locations, weathering of very coarse grained peridotite is characterized by a green-brown weathered surface. In other places, these rocks can be identified by typical spheroidal weathering, of which the final product is brown soil. This is consistent with the field observations of Larocque and Canil (2006).

All outcrops of the layered intrusions have an average strike of  $040 \pm 20^\circ$  and a dip of  $50 \pm 10^\circ$  southeast. Other igneous rock types in the area are fine- to coarse-grained gabbro–hornblende gabbro, fine- to medium-grained diorite, tonalite and plagioclase-phyrlic dacite.

Joint sets and local faults are the major structures in the area. These strike approximately southeast and dip steeply southwest. Local faults are very narrow with slickensided surfaces, with or without fault gouge. They strike west-northwest and southwest and dip steeply north-northeast and northwest, respectively. The trend and plunge of the slickensides implies horizontal movement along these faults, but no offsets were observed. These faults and horizontal movements along them reflect local adjustments of blocks as a response to the current transpressional regime.

In the southernmost portion of the study area, a 20 m wide shear zone with cataclastic-mylonitic fabric trends east. Due to strong deformation along the shear zone, the sheared rock cannot be identified with any confidence. However, the chloritic, green appearance of the shear zone and gradual transition into a very coarse grained peridotite and medium-grained gabbro imply that shear might have occurred preferentially along the ultramafic body. The zone is heavily fractured, veined and chloritized. A portion of sheared gabbro shows plagioclase replaced by epidote and

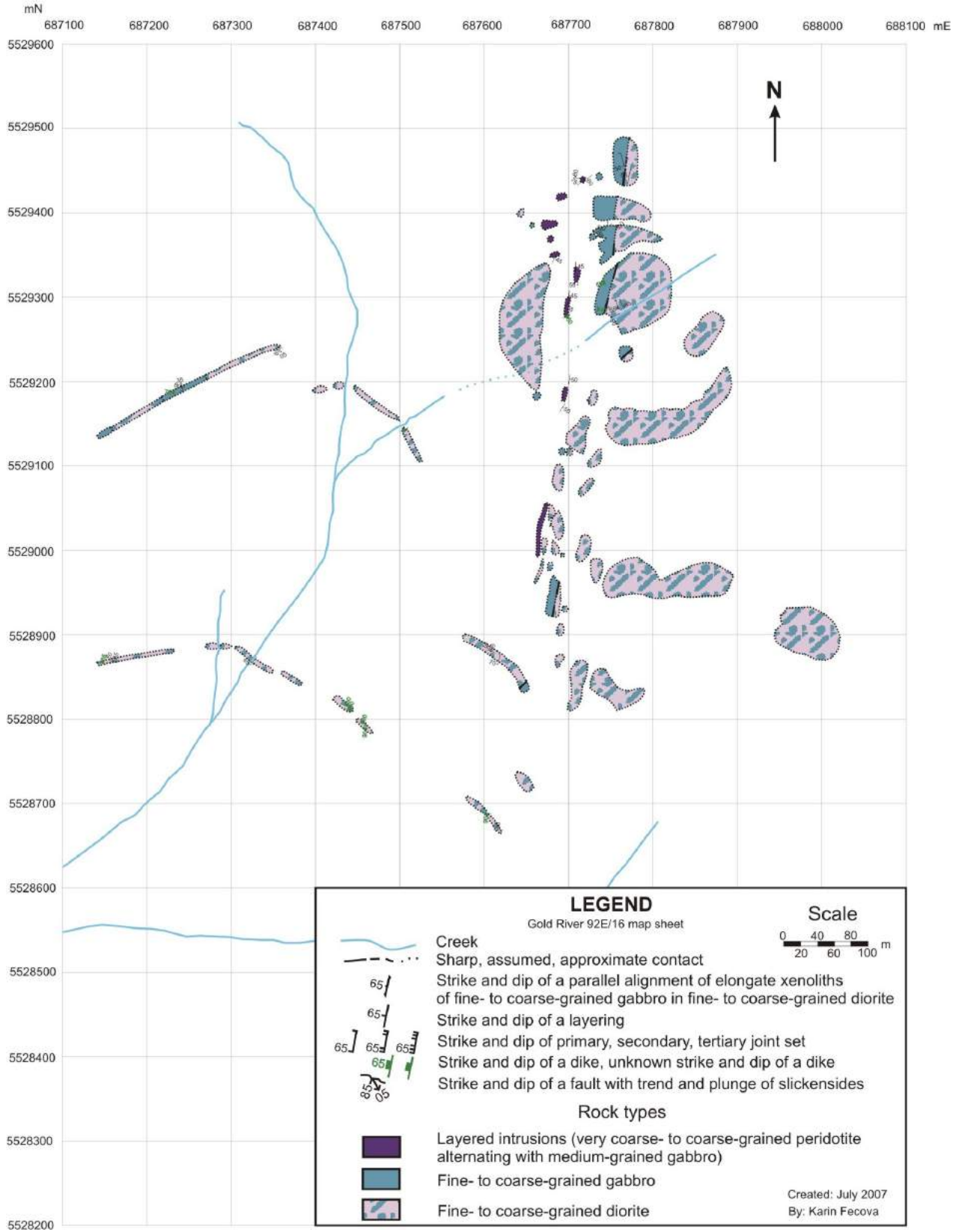
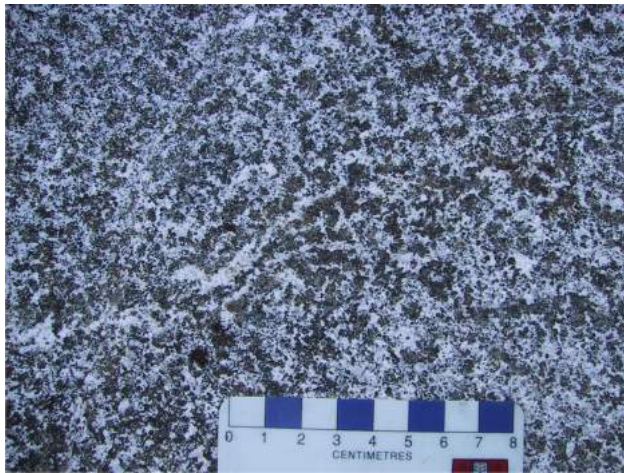


Figure 2. Detailed geology of layered intrusions in the Conuma River area. Location marked by the black rectangle on Figure 1.



**Figure 3.** Very coarse grained peridotite from the Conuma River area. This unit is distinctive in the field, characterized by the tan colour, strong magnetism and pitted weathered surface with out-lines of pyroxene-hornblende megacrysts.



**Figure 4.** Medium-grained gabbro from the Conuma River area. The unit displays typical white–light grey weathering colour and is associated with both the layered intrusions and the gabbroic units outward from the layered intrusions.

2–4 mm garnet crystals that are likely a product of metasomatism during shearing. A plagioclase-phyric dacite dike, about 50 cm wide, parallels the shear zone and appears to be unaffected by the shear. This type of dike is common in the study area and contains 15% randomly distributed, euhedral plagioclase phenocrysts (2–15 mm) and 5% black hornblende phenocrysts (1–3 mm) in a green-gray dacitic groundmass. The plagioclase phenocrysts were separated and dated by Ar-Ar. The results do not yield a well-defined plateau but favour a Jurassic rather than Eocene age.

### Unit Description of Layered Intrusions

The Conuma phase (Marshall et al., 2006) of the Island Intrusive Suite consists of two major rock types, as previously mentioned. These are medium-grained gabbro and

very coarse to coarse-grained peridotite. The peridotite is tan weathering and dark green-black on fresh surfaces, with 40% euhedral, unaltered olivine (millimetre size), enclosed in 45% poikilitic orthopyroxene (20 mm) and 10% poikilitic hornblende (20 mm). Minor constituents are phlogopite, plagioclase and magnetite. The unit is strongly magnetic. Considering hornblende as an alteration product of pyroxene, the original rock type was probably olivine websterite.

The medium-grained gabbro weathers a light brownish green and is dark green-grey on the fresh surface. It is an equigranular holocrystalline rock with 60% euhedral green hornblende (3 mm) and 40% euhedral white plagioclase (3 mm). The unit is weakly magnetic, with sulphide minerals locally ranging up to 5%.

### Contact Relationships

Layered intrusions outcrop as isolated blocks that appear discontinuous due to vegetation and Quaternary cover. No tectonic or intrusive contacts between the layered intrusions and country rocks have been observed. Nor has any lateral or vertical continuity been observed between individual outcrops. The layered peridotite unit is observed in a number of outcrops, either exclusively or as cyclic units of very coarse grained peridotite and medium-grained gabbro. Repetition of both units occurs on a scale of approximately 20 cm. The layering is not as obvious at adjacent outcrops, but it is still occasionally present in the coarse- and medium-grained gabbros. This less distinctive layering is probably due to a subtle modal and grain-size change within a single unit. Gabbro with less distinctive layering grades into nonlayered gabbro with variable grain sizes and modal abundances. Where the plagioclase content in nonlayered gabbro increases, it results in hornblende gabbro and hornblende diorite. Patches, pods, lenses, zones and bands of hornblende gabbro and hornblende diorite at the centimetre to metre scale are common in the nonlayered gabbro (Figures 5 and 6). The nonlayered gabbro is in sharp contact with a medium-grained diorite intrusion that intrudes the gabbro. The contact between gabbro and the diorite intrusion was observed in three outcrops and tends to have a general northerly trend that is subparallel to the strike of the layers within the layered intrusions.

Contacts within the layered intrusions and with the nonlayered gabbro are abrupt and are based on differences in grain size and/or phase abundances. Contacts between layers follow a generally planar trend with local irregularities. Contacts between tonalitic dikes and ultramafic/mafic rocks are sharp. Contacts between medium-grained diorite and ultramafic/mafic rocks are dominantly sharp. Contacts between tonalite and medium-grained diorite are also dominantly sharp.

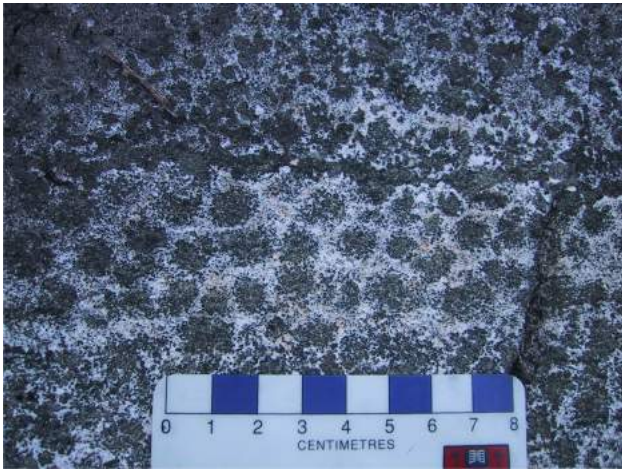


**Figure 5.** Coarse-grained hornblende gabbro from the Conuma River area. This unit is characterized by well-developed hornblende crystals surrounded by plagioclase, giving the rock a mottled appearance.



**Figure 6.** Pegmatitic pod, consisting of well-developed hornblende and plagioclase crystals. These pods are very common features in medium-grained gabbro and occur randomly within this unit.

### Textural and Structural Features

The cumulate texture in the peridotite is characterized by cumulate olivine crystals in intercumulus crystals of pyroxene and hornblende. Plagioclase, if present, is also intercumulate. Field observations indicate that crystal settling by gravity was one of the depositional mechanisms during formation of the layered intrusions. The presence of magmatic density currents in the magma chamber during crystallization of the ultramafic magma is exhibited by features that resemble soft-sediment deformation and convoluted bedding (Irvine, 1980). Surfaces of the medium-grained gabbro layers with already-settled crystals appear to be disturbed by layers of very coarse grained peridotite similar to scour marks in sedimentary rocks. The disruption of a partially molten gabbro layer can result in partial or

complete separation into a gabbro layer and a dense peridotite crystal mush. These separated or disrupted portions then have the shape of lenses, pods and swirls, which are usually visible at outcrop scale (Figures 7 and 8).

### Geochronology

Marshall et al. (2006) published results of Ar-Ar hornblende dating of the very coarse grained peridotite unit. The dating suggests that the ultramafic intrusions are of Jurassic age ( $189.9 \pm 2.1$  Ma). Additional  $^{40}\text{Ar}$ - $^{39}\text{Ar}$  data obtained from the Jurassic intrusions (Figure 1) are listed in Tables 1 to 4, and the corresponding spectra are shown in Figure 9.



**Figure 7.** Layered ultramafic intrusions in the Conuma River area, showing soft-sediment-like deformation of the medium-grained gabbro unit.



**Figure 8.** Detail of the convoluted bedding observed in the medium-grained gabbro and very coarse grained peridotite within layered intrusions of the Conuma River area. According to Irvine (1974), the convoluted layering is a result of deformation of crystal-mush layers during emplacement.

**Table 1.**  $^{40}\text{Ar}$ - $^{39}\text{Ar}$  data from sample DM05-20 ( $190.3 \pm 1.4$  Ma), Jurassic Island Intrusive Suite.

Laser power (%)	Isotope Ratios								Age	
	$^{40}\text{Ar}/^{39}\text{Ar}$	$^{38}\text{Ar}/^{39}\text{Ar}$	$^{37}\text{Ar}/^{39}\text{Ar}$	$^{36}\text{Ar}/^{39}\text{Ar}$	Ca/K	Cl/K	% $^{40}\text{Ar}$ atm <sup>(1)</sup>	f $^{39}\text{Ar}$ <sup>(2)</sup>		$^{40}\text{Ar}^*/^{39}\text{ArK}$
2	783.638 ±0.054	3.629 ±0.075	2.653 ±0.086	2.373 ±0.057	15.34	0.761	81.15	0.13	149.209 ±17.137	1063.77 ±92.30
2.3	192.647 ±0.022	1.334 ±0.031	2.984 ±0.039	0.616 ±0.038	22.82	0.282	84.21	0.47	29.627 ±5.940	267.00 ±49.76
2.6	108.549 ±0.018	0.760 ±0.025	2.679 ±0.039	0.329 ±0.032	21.39	0.159	81.81	1.18	19.321 ±2.662	178.54 ±23.42
2.9	43.037 ±0.009	0.804 ±0.017	2.058 ±0.023	0.105 ±0.029	16.66	0.179	62.91	2.94	15.534 ±0.910	144.90 ±8.16
3.2	31.844 ±0.012	1.415 ±0.016	2.511 ±0.018	0.040 ±0.026	20.37	0.324	28.26	5.86	22.489 ±0.447	206.19 ±3.87
3.5	23.792 ±0.014	1.802 ±0.016	2.681 ±0.018	0.015 ±0.034	21.88	0.415	12.18	20.12	20.843 ±0.349	191.88 ±3.05
3.8	23.020 ±0.013	1.925 ±0.014	2.935 ±0.017	0.013 ±0.027	23.98	0.444	9.19	23.64	20.890 ±0.300	192.29 ±2.62
4.1	22.729 ±0.014	1.917 ±0.017	3.069 ±0.021	0.014 ±0.021	25.06	0.442	9.36	14.75	20.501 ±0.318	188.89 ±2.78
4.4	21.839 ±0.005	1.762 ±0.012	2.520 ±0.014	0.010 ±0.048	20.51	0.405	4.63	11.55	20.610 ±0.183	189.84 ±1.60
5	22.162 ±0.016	1.821 ±0.020	2.821 ±0.021	0.011 ±0.043	23.03	0.419	7.01	19.36	20.546 ±0.364	189.28 ±3.18
Total/avg.	26.380 ±0.003	1.783 ±0.003	12.273 ±0.002	0.023 ±0.006		0.383		100	20.570 ±0.075	

<sup>(1)</sup> percentage of  $^{40}\text{Ar}$  in the analyzed gas fraction

<sup>(2)</sup> percentage of  $^{39}\text{Ar}$  released relative to the total amount of  $^{39}\text{Ar}$  released from the sample

Flux correction factor (J) = 0.005384 ±0.000006

Volume  $^{39}\text{ArK}$  = 157.32

Integrated date = 191.97 ±1.32

Volumes are  $1 \times 10^{-13} \text{ cm}^3$  at normal pressure and temperature

Neutron flux monitors: 28.02 Ma FCs (Fish Canyon sanidine; Renne et al., 1998)

Isotope production ratios: ( $^{40}\text{Ar}/^{39}\text{Ar}$ )K = 0.0302 ±0.00006; ( $^{37}\text{Ar}/^{39}\text{Ar}$ )Ca = 1416.4 ±0.5; ( $^{36}\text{Ar}/^{39}\text{Ar}$ )Ca = 0.3952 ±0.0004; Ca/K = 1.83 ±0.01 ( $^{37}\text{ArCa}/^{39}\text{ArK}$ ).

**Table 2.**  $^{40}\text{Ar}$ - $^{39}\text{Ar}$  data from sample DM05-212A ( $189.9 \pm 2.1$  Ma), Jurassic Island Intrusive Suite.

Laser power (%)	Isotope Ratios								Age	
	$^{40}\text{Ar}/^{39}\text{Ar}$	$^{38}\text{Ar}/^{39}\text{Ar}$	$^{37}\text{Ar}/^{39}\text{Ar}$	$^{36}\text{Ar}/^{39}\text{Ar}$	Ca/K	Cl/K	% $^{40}\text{Ar}$ atm <sup>(1)</sup>	f $^{39}\text{Ar}$ <sup>(2)</sup>		$^{40}\text{Ar}^*/^{39}\text{ArK}$
2	3548.409 ±0.168	8.734 ±0.183	8.658 ±0.195	10.238 ±0.171	36.91	2.108	73.58	0.02	1222.646 ±367.349	3653.98 ±470.53
2.4	1575.382 ±0.050	4.205 ±0.067	5.494 ±0.056	4.317 ±0.054	37.95	0.829	75.44	0.13	405.209 ±36.995	2087.36 ±112.92
2.8	612.327 ±0.038	1.705 ±0.051	4.157 ±0.052	1.829 ±0.043	30.21	0.319	81.1	0.27	116.513 ±13.453	878.07 ±80.27
3.2	60.232 ±0.011	0.881 ±0.020	4.046 ±0.021	0.137 ±0.033	32.95	0.196	59.36	3.93	24.210 ±1.389	220.93 ±11.93
3.6	32.541 ±0.015	0.701 ±0.022	3.396 ±0.019	0.041 ±0.035	27.72	0.158	28.54	10.39	23.085 ±0.577	211.24 ±4.98
4	25.486 ±0.013	0.609 ±0.018	2.885 ±0.018	0.021 ±0.031	23.57	0.137	18.05	33.23	20.891 ±0.359	192.19 ±3.13
4.4	23.103 ±0.016	0.575 ±0.019	3.095 ±0.021	0.015 ±0.036	25.29	0.13	11.01	23.81	20.508 ±0.383	188.85 ±3.35
5	23.162 ±0.015	0.727 ±0.018	3.154 ±0.020	0.015 ±0.032	25.78	0.165	11.61	28.21	20.456 ±0.363	188.39 ±3.18
Total/avg.	30.805 ±0.003	0.665 ±0.005	13.766 ±0.003	0.034 ±0.006		0.505		100	20.640 ±0.108	

<sup>(1)</sup> percentage of  $^{40}\text{Ar}$  in the analyzed gas fraction

<sup>(2)</sup> percentage of  $^{39}\text{Ar}$  released relative to the total amount of  $^{39}\text{Ar}$  released from the sample

Flux correction factor (J) = 0.005381 ±0.000006

Volume  $^{39}\text{ArK}$  = 117.79

Integrated date = 202.46 ±1.89

Volumes are  $1 \times 10^{-13} \text{ cm}^3$  at normal pressure and temperature

Neutron flux monitors: 28.02 Ma FCs (Fish Canyon sanidine; Renne et al., 1998)

Isotope production ratios: ( $^{40}\text{Ar}/^{39}\text{Ar}$ )K = 0.0302 ±0.00006; ( $^{37}\text{Ar}/^{39}\text{Ar}$ )Ca = 1416.4 ±0.5; ( $^{36}\text{Ar}/^{39}\text{Ar}$ )Ca = 0.3952 ±0.0004; Ca/K = 1.83 ±0.01 ( $^{37}\text{ArCa}/^{39}\text{ArK}$ ).

**Table 3.**  $^{40}\text{Ar}$ - $^{39}\text{Ar}$  data from sample DM05-162 ( $176.4 \pm 1.3$  Ma), Jurassic Island Intrusive Suite.

Laser power (%)	Isotope Ratios								Age	
	$^{40}\text{Ar}/^{39}\text{Ar}$	$^{38}\text{Ar}/^{39}\text{Ar}$	$^{37}\text{Ar}/^{39}\text{Ar}$	$^{36}\text{Ar}/^{39}\text{Ar}$	Ca/K	Cl/K	% $^{40}\text{Ar}$ atm <sup>(1)</sup>	f $^{39}\text{Ar}$ <sup>(2)</sup>		$^{40}\text{Ar}^*/^{39}\text{ArK}$
2	579.288 ±0.038	3.338 ±0.046	1.048 ±0.116	1.465 ±0.057	3.031	0.712	66.19	0.18	189.228 ±20.368	1267.21 ±97.99
2.4	139.154 ±0.018	0.880 ±0.035	0.794 ±0.048	0.355 ±0.041	5.429	0.186	66.87	0.77	44.286 ±3.992	385.74 ±31.31
2.8	45.711 ±0.007	0.572 ±0.022	1.879 ±0.020	0.097 ±0.035	15.93	0.125	54.45	3.23	20.271 ±0.994	186.84 ±8.70
3.2	24.726 ±0.010	1.523 ±0.014	2.317 ±0.016	0.021 ±0.026	20.05	0.349	19.45	31.47	19.902 ±0.260	183.61 ±2.28
3.5	21.336 ±0.006	1.490 ±0.012	2.302 ±0.015	0.012 ±0.021	19.91	0.342	10.48	30.88	19.063 ±0.141	176.24 ±1.24
3.8	21.246 ±0.014	1.656 ±0.014	2.413 ±0.017	0.013 ±0.034	20.86	0.381	10.23	16.69	18.934 ±0.317	175.10 ±2.80
4.1	21.832 ±0.006	1.593 ±0.010	2.456 ±0.014	0.014 ±0.056	21.41	0.366	11.17	15.17	19.240 ±0.262	177.79 ±2.30
4.5	20.999 ±0.013	1.565 ±0.023	3.318 ±0.021	0.044 ±0.079	28.44	0.36	22.89	1.61	14.182 ±1.050	132.72 ±9.48
Total/avg.	24.782 ±0.002	1.514 ±0.003	10.956 ±0.002	0.020 ±0.007		0.353		100	19.240 ±0.066	

<sup>(1)</sup> percentage of  $^{40}\text{Ar}$  in the analyzed gas fraction

<sup>(2)</sup> percentage of  $^{39}\text{Ar}$  released relative to the total amount of  $^{39}\text{Ar}$  released from the sample

Flux correction factor (J) = 0.005383 ±0.000006

Volume  $^{39}\text{ArK}$  = 135.01

Integrated date = 182.89 ±1.17

Volumes are  $1 \times 10^{-13} \text{ cm}^3$  at normal pressure and temperature

Neutron flux monitors: 28.02 Ma FCs (Fish Canyon sanidine; Renne et al., 1998)

Isotope production ratios: ( $^{40}\text{Ar}/^{39}\text{Ar}$ )K = 0.0302 ±0.00006; ( $^{37}\text{Ar}/^{39}\text{Ar}$ )Ca = 1416.4 ±0.5; ( $^{36}\text{Ar}/^{39}\text{Ar}$ )Ca = 0.3952 ±0.0004; Ca/K = 1.83 ±0.01 ( $^{37}\text{ArCa}/^{39}\text{ArK}$ ).

Table 4.  $^{40}\text{Ar}$ - $^{39}\text{Ar}$  data from sample DM05-121 (169.3 ± 1.2 Ma), Jurassic Island Intrusive Suite.

Laser power (%)	Isotope Ratios							Age		
	$^{40}\text{Ar}/^{39}\text{Ar}$	$^{38}\text{Ar}/^{39}\text{Ar}$	$^{37}\text{Ar}/^{39}\text{Ar}$	$^{36}\text{Ar}/^{39}\text{Ar}$	Ca/K	Cl/K	% $^{40}\text{Ar}$ atm <sup>(1)</sup>			
2	546.915 ± 0.101	1.222 ± 0.185	1.685 ± 0.169	1.851 ± 0.127	9.494	0.208	78.26	0.06	91.420 ± 53.372	721.32 ± 347.11
2.3	225.262 ± 0.018	0.357 ± 0.144	0.498 ± 0.102	0.721 ± 0.035	4.915	0.048	88.55	0.5	23.603 ± 6.478	215.56 ± 55.76
2.6	102.643 ± 0.014	0.157 ± 0.083	0.444 ± 0.068	0.317 ± 0.042	5.489	0.019	87.19	1.72	12.382 ± 3.715	116.29 ± 33.79
2.9	52.055 ± 0.017	0.123 ± 0.066	0.401 ± 0.082	0.172 ± 0.068	4.696	0.017	86.01	1.24	6.091 ± 3.376	58.14 ± 31.71
3.2	29.102 ± 0.006	0.264 ± 0.026	0.560 ± 0.027	0.067 ± 0.026	7.463	0.055	61.31	6.17	10.594 ± 0.506	99.95 ± 4.65
3.5	20.903 ± 0.007	0.949 ± 0.012	1.422 ± 0.016	0.017 ± 0.028	19.36	0.216	15.65	19.07	17.247 ± 0.182	159.99 ± 1.62
3.8	22.036 ± 0.007	0.774 ± 0.016	1.224 ± 0.031	0.020 ± 0.080	16.52	0.175	10.37	5.18	18.012 ± 0.501	166.78 ± 4.43
4.1	20.470 ± 0.005	1.082 ± 0.011	1.592 ± 0.014	0.012 ± 0.030	21.72	0.248	9.21	28.44	18.350 ± 0.143	169.76 ± 1.26
4.4	19.937 ± 0.005	1.029 ± 0.012	1.538 ± 0.013	0.010 ± 0.042	21.15	0.235	7.12	27.37	18.257 ± 0.156	168.94 ± 1.38
5	19.920 ± 0.008	0.929 ± 0.015	1.455 ± 0.024	0.016 ± 0.035	19.9	0.212	6.51	6.48	17.200 ± 0.229	159.58 ± 2.04
5.5	37.801 ± 0.010	0.737 ± 0.025	1.151 ± 0.024	0.082 ± 0.039	15.6	0.164	55.12	3.78	15.781 ± 0.933	146.94 ± 8.34
Total/avg.	23.659 ± 0.001	0.921 ± 0.003	10.322 ± 0.001	0.025 ± 0.008		0.145		100	18.279 ± 0.064	

<sup>(1)</sup> percentage of  $^{40}\text{Ar}$  in the analyzed gas fraction

<sup>(2)</sup> percentage of  $^{39}\text{Ar}$  released relative to the total amount of  $^{39}\text{Ar}$  released from the sample

Flux correction factor (J) = 0.005377 ± 0.000006

Volume  $^{39}\text{ArK}$  = 94.21

Integrated date = 160.13 ± 1.15

Volumes are  $1 \times 10^{-13} \text{ cm}^3$  at normal pressure and temperature

Neutron flux monitors: 28.02 Ma FCs (Fish Canyon sanidine; Renne et al., 1998)

Isotope production ratios: ( $^{40}\text{Ar}/^{39}\text{Ar}$ )K = 0.0302 ± 0.00006; ( $^{37}\text{Ar}/^{39}\text{Ar}$ )Ca = 1416.4 ± 0.5; ( $^{36}\text{Ar}/^{39}\text{Ar}$ )Ca = 0.3952 ± 0.0004, Ca/K = 1.83 ± 0.01 ( $^{37}\text{ArCa}/^{39}\text{ArK}$ ).

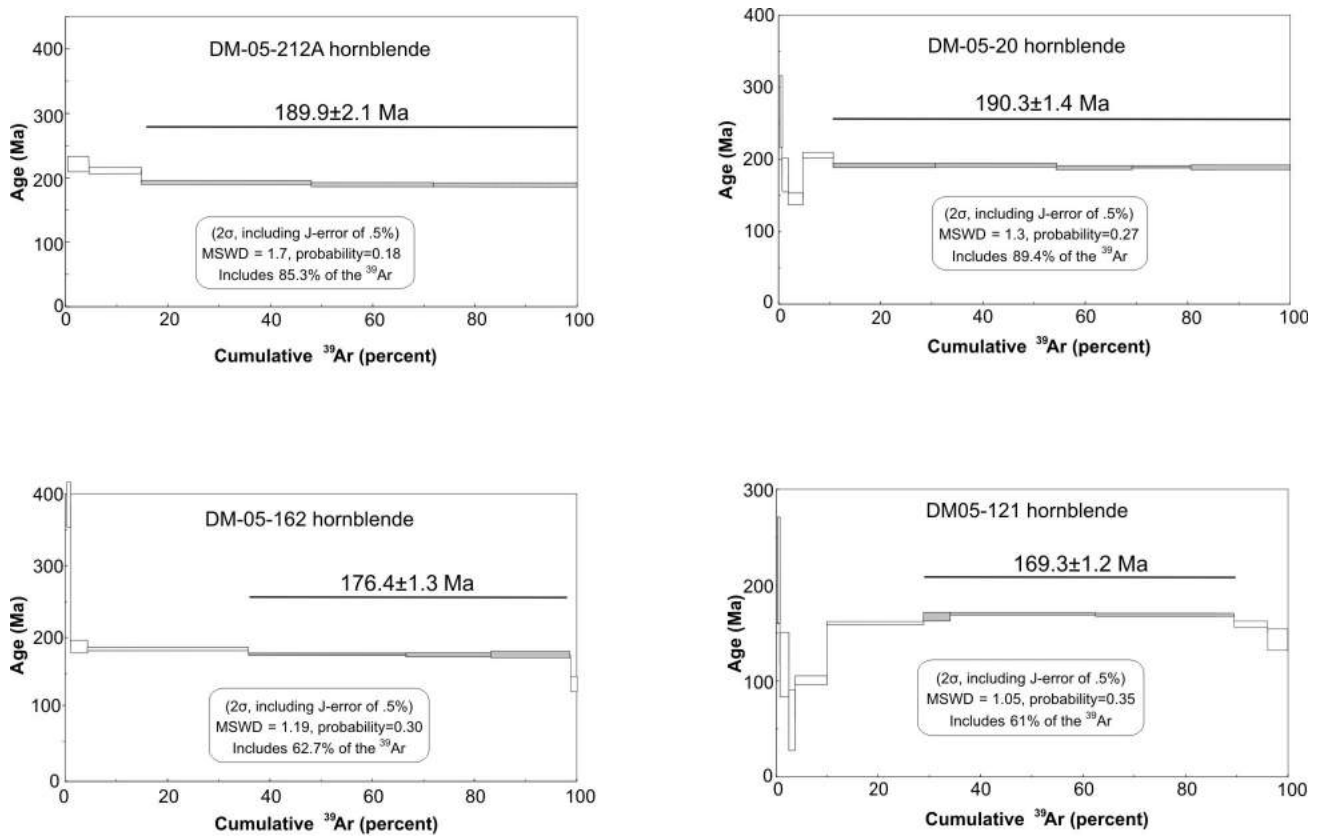


Figure 9.  $^{40}\text{Ar}$ - $^{39}\text{Ar}$  gas release spectra of four samples from the Jurassic Island Intrusive Suite, corresponding to the data in Table 1. All samples yield Jurassic plateaus.

## Mafic Rocks and Local Geology of the Norgate Creek Area

Mafic intrusions of the Norgate Creek area are continuous outcrops of steep cliffs that can be followed for up to a kilometre. This area shows both horizontally and vertically layered intrusions.

Horizontally layered intrusions exhibit layers at centimetre to millimetre scale and consist of one rock type, a fine- to medium-grained gabbro that consists of approximately 40% plagioclase and 60% pyroxene ( $\pm$ hornblende) crystals. Layers are planar, well defined at outcrop scale and probably visible due to differential weathering (Figure 10).

Lateral change along the outcrop cliffs is marked by irregular and abrupt contacts due to changes in modal compositions. No repetition in cyclic units or sedimentary-type structures were observed in these mafic rocks at the outcrop scale. Common rock types are very fine, fine- and medium-grained gabbro and hornblende gabbro. A scanning electron microscope image of well-developed and abundant magnetite grains from a medium-grained hornblende gabbro unit was published by Marshall et al. (2006). Besides the magnetite abundance, interesting replacement textures are also present in this gabbroic unit. The unit weathers dark grey and is black on fresh surfaces and equigranular, consisting of 60% intercumulus hornblende with pyroxene cores, 30% cumulus plagioclase and 10% cumulus olivine that is completely altered to serpentine. The sample in thin section shows a high degree of alteration (Figure 11).

Individual gabbro types can be traced across different outcrops. These gabbro units intrude the Mooyah Formation, which is strongly hornfelsed due to contact metamorphism. The hornfelsed Mooyah Formation contains up to 20% sulphide minerals. No massive diorite intrusions were found in the Norgate Creek area.



**Figure 10.** Fine layering in the gabbroic rocks from the Norgate Creek area. The layering is best observed on the weathered surface.

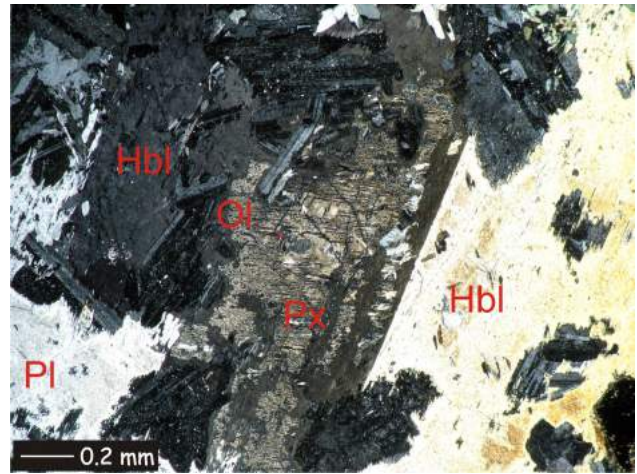


**Figure 11.** Photomicrograph of medium-grained hornblende gabbro from the Norgate Creek area. Olivine altered to serpentine and saussuritized plagioclase are cumulus crystals within intercumulus zones of serpentinized pyroxene with fresh hornblende rims. Low interference colours (crossed polars) are due to thinning of the thin section at its edge.

## Ultramafic and Mafic Rocks, and Local Geology of the Cypress Creek Area

The Cypress Creek area is characterized by isolated ultramafic bodies within mafic phases of medium-grained diorite and by the presence of a very distinctive ultramafic breccia (Figure 12).

The mafic unit is a coarse-grained olivine gabbro. It is black on the weathered surface and greenish black on the fresh surface. It consists of 80% hornblende/pyroxene crystals (5–15 mm) enclosing 10% anhedral olivine crystals (1 mm) and 10% altered plagioclase (5–8 mm). The unit is strongly magnetic.



**Figure 12.** Ultramafic breccia from the Cypress Creek area shows a very distinctive brecciation of ultramafic rocks into angular clasts. Sulphide-rich mineralized clasts are chloritized peridotite and coarse-grained gabbro enclosed in a leucocratic matrix of quartz and plagioclase.

The outcrop of ultramafic breccia is 150 m long and trends northeast. Medium-grained diorite intrudes Karmutsen volcanic rocks and peridotite at its northeast end. Diorite dikes brecciate peridotite in the central portion of the outcrop and tonalite dikes brecciate peridotite at its southwest end. The ultramafic breccia consists of 10–50 cm, angular to rounded, deformed, fragmented, heavily veined, rusty-weathering and dark green fresh peridotite clasts. Very coarse grained peridotite is composed of 50% intercumulus hornblende or pyroxene (15–20 mm), 45% cumulus olivine crystals (1 mm) and 5% intercumulus plagioclase (2 mm). This unit is magnetic, with up to 15–20% sulphide clusters consisting of crystals of pyrrhotite and other sulphide minerals (up to 10 mm). Sulphide clusters were also found within the dikes.

Medium- to coarse-grained equigranular hornblende diorite intruding ultramafic rocks weathers dark grey and is black and white on the fresh surface, with 50% hornblende crystals (2–3 mm) and 50% plagioclase crystals (2–3 mm).

### Ultramafic Rocks and Local Geology of the Leagh Creek Area

Pyroxene-hornblende gabbro is dark grey on fresh and weathered surfaces. It is a medium-grained rock with 40–45% prismatic, euhedral black pyroxene and dark green hornblende crystals (1–2 mm), 55–60% subhedral plagioclase crystals (1–2 mm) and approximately 2% sulphide minerals. This gabbro is magnetic with millimetre- to centimetre-size feldspar-quartz-epidote alteration veins. The gabbro is also intruded by medium-grained hornblende diorite and by north-striking, moderately dipping andesitic dikes. The andesite weathers a medium grey-green and is medium grey on the fresh surface. It is recrystallized in some locations, comprising 1 mm grains of plagioclase, quartz and altered hornblende with occasional phenocrysts of black idiomorphic pyroxene. It contains up to 2% sulphide minerals.

### Potential for Platinum-Group-Element Mineralization

Platinum-group-element (PGE) mineralization in layered intrusions associated with continental magmatism has been observed in a number of localities worldwide, such as the Bushveld and Stella in South Africa, the Stillwater in the United States and many other layered intrusions (Prendergast, 2000; Maier et al., 2003). All have a tholeiitic chemical signature and represent two types of layered intrusion with PGE mineralization. The ‘Bushveld type’ is a large intrusion with PGE mineralization at deeper levels, where the PGEs are associated with chromite. The ‘Stella type’ is a small intrusion in which PGE mineralization is found at shallow levels and in association with magnetite (Maier et al., 2003). Although the Conuma layered ultramafic rocks are more likely associated with island-arc

magmatism, they may still be prospective for Stella-type PGE mineralization.

Marshall et al. (2006) published Pt, Pd, Au and Cu analyses from the magnetite-rich sample of the medium-grained hornblende gabbro intrusion from the Norgate Creek area. The values reported were relatively low, compared to a sample of fine-grained, nonmagnetic gabbro from the same area, collected and assayed by prospector E. Specogna. Mr. Specogna released assay results in his open file report, which shows anomalous values for Pt, Pd and Ni (Specogna and Specogna, 2003).

Platinum-group-element mineralization can be correlative with Ni, Au and Cu, and can be also associated with magnetite or chromite (Prendergast, 2000; Maier et al., 2003). Understanding the conditions of crystallization in the magma chamber and considering a presence and/or absence of certain minerals/metals can lead to a reasonable interpretation of PGE precipitation depths within the Conuma River and Norgate Creek intrusions. The elements Os, Ir, Ru and Rh behave as compatible elements and tend to partition into spinel or olivine during early stages of magma crystallization, and thus tend to be concentrated in deeper portions of intrusions. The elements Pt, Pd, Cu and Au can also precipitate during early crystallization of magma and associate with chromite. If the magma is S-undersaturated, these elements behave incompatibly and tend to stay in the melt until the magma reaches S and Fe-oxide saturation. Then they precipitate in association with magnetite with (or without) sulphide minerals during the later stages of magma crystallization at shallow levels (Maier et al., 2003). Additional geochemical studies are underway to further evaluate the PGE potential of these rocks.

The Conuma layered intrusions are magnetite rich, especially the very coarse to coarse-grained peridotite unit, and they may represent shallow levels of an intrusion. It is believed that PGE mineralization at shallow levels favours a contribution from mantle melts, especially mantle plumes and involvement of crustal assimilation. A lack of crustal assimilation can result in early S saturation and PGE precipitation at a deeper level within the intrusion (Maier et al., 2003). The geochronology of the Conuma ultramafic rocks is consistent with the emplacement of the Jurassic Island Intrusive Suite. Thus, there is the possibility that PGE elements could precipitate both at deeper levels within the intrusion (due to arc crust contamination) and at shallow levels (due to association with magnetite-rich layers).

## Discussion

Jackson (1971) summarized information on different types of ultramafic intrusions worldwide. The closest analogy to Conuma layered intrusions is ‘Alaskan peridotite’, which also has analogues in the Urals, Russia and in the Tulameen

region of BC. These ultramafic intrusions share similar characteristics, such as

- being restricted to island arcs;
- synorogenic or postorogenic emplacement;
- association with andesitic volcanism or granodioritic intrusions;
- development of a metamorphic aureole;
- cylindrical zonation, with ultramafic rocks in the centre grading outward to mafic and intermediate rocks such as gabbro, tonalite and granodiorite;
- the presence of olivine, clinopyroxene and magnetite;
- magnetite-rich pyroxenite dikes;
- amphibolitized border rocks; and
- PGE enrichment.

According to Taylor and Noble (1969) 'Alaskan peridotites' represent cumulates from ultramafic melts, forming in unstable environments with multiple injections of ultramafic crystal mush that mixes prior solidification. The occurrence of ultramafic rocks with gabbros, diorites and granodiorites suggests that these rocks formed from ultramafic melts of alkaline basaltic or andesitic parentage (Jackson, 1971).

Irvine (1967) showed a number of images of folded intrusion layers, soft-sediment-like deformation of intrusion layers, crossbedding and scours in layered intrusions. The deformation and mineralogy of the Conuma ultramafic rocks resembles some of Irvine's images and rock types.

The Tulameen ultramafic-gabbro complex described by Findlay (1969) represents a nonstratiform type of ultramafic intrusion in which ultramafic intrusions intrude each other. This type more closely resembles observations from the Norgate ultramafic intrusions, which record at least four intrusive events.

Larocque and Canil (2006) reported a mica peridotite unit from the Port Renfrew area on Vancouver Island. Lithological and petrographic description, as well as the association of mica peridotite with rocks of the Island Intrusive Suite, implies a similar genesis for the Conuma and Port Renfrew ultramafic rocks. It also implies that there may be many more ultramafic bodies and intrusions between Conuma and Port Renfrew that would be prospective for PGE and Ni mineralization.

Ultramafic and mafic intrusions from the Gold River study area will be examined in detail using data from whole-rock and mineral geochemistry in a manner similar to studies in the Border Ranges of Alaska by Burns (1985) and DeBari and Coleman (1989). Magma-fractionation modelling will be used to find the composition of parent magmas responsible for crystallization of ultramafic rocks and to find any fractionation trends within the layered intrusions and/or a petrological relationship to the Jurassic diorite and

granodiorite. This study will also focus on interpretation of crystallization history, mechanisms responsible for cumulate textures and emplacement of the layered intrusions.

## Acknowledgments

The authors are very grateful to Geoscience BC for supporting the project financially and for a student scholarship to the senior author. The authors would also like to thank to E. Specogna and Hard Creek Nickel Corporation for property access. N. Massey from the British Columbia Geological Survey is thanked for comments and improvements to an earlier version of this manuscript.

## References

- BC Geological Survey (2007): MapPlace GIS internet mapping system; BC Ministry of Energy, Mines and Petroleum Resources, MapPlace website, URL <<http://www.MapPlace.ca>> [November 2007].
- Burns, L.E. (1985): The Border Ranges ultramafic and mafic complex, south-central Alaska: cumulate fractionates of island-arc volcanics; *Canadian Journal of Earth Sciences*, v. 22, p. 1020–1038.
- Close, S. (2006): Geology and tectonics of the Nootka Island region, British Columbia; M.Sc. thesis, Simon Fraser University, Burnaby, BC, 96 p.
- DeBari, S.M. and Coleman, R.G. (1989): Examination of the deep levels of an island arc: evidence from the Tonsina ultramafic-mafic assemblage, Tonsina, Alaska; *Journal of Geophysical Research*, v. 94, no. B4, p. 4373–4391.
- DeBari, S.M., Anderson, R.G. and Mortensen, J.K. (1999): Correlation among lower to upper crustal components in an island arc: the Jurassic Bonanza arc, Vancouver Island, Canada; *Canadian Journal of Earth Sciences*, v. 36, p. 1371–1413.
- Findlay, D.C. (1969): Origin of the Tulameen ultramafic-gabbro complex, southern British Columbia; *Canadian Journal of Earth Sciences*, v. 6, p. 399–425.
- Irvine, T.N. (1974): Petrology of the Duke Island Ultramafic Complex, southeastern Alaska; *Geological Society of America, Memoir* 138, 240 p.
- Irvine, T.N. (1980): Magmatic density currents and cumulus processes; *American Journal of Science*, v. 280-A, p. 1–58.
- Isachsen, C.E. (1987): Geology, geochemistry, and cooling history of the Westcoast Crystalline Complex and related rocks, Meares Island and vicinity, Vancouver Island, British Columbia; *Canadian Journal of Earth Sciences*, v. 24, p. 2047–2064.
- Jackson, E.D. (1971): The origin of ultramafic rocks by cumulus processes; *Fortschritte der Mineralogie*, v. 48, no. 1, p. 128–174.
- Larocque, J. and Canil, D. (2007): Ultramafic rock occurrences in the Jurassic Bonanza Arc near Port Renfrew (NTS 092C/09, 10, 15, 16), southern Vancouver Island; *in Geological Fieldwork 2006*, BC Ministry of Energy, Mines and Petroleum Resources, Paper 2007-1 and Geoscience BC, Report 2007-1, p. 319–324.
- Maier, W.D., Barnes, S.J., Gartz, V. and Andrews G. (2003): Pt-Pd reefs in magnetites of the Stella layered intrusions, South Africa: a world of new exploration opportunities for plati-

- num group elements; Geological Society of America, v. 31, no. 10, p. 885–888.
- Marshall, D., Lesiczka, M., Xue, G., Close, S. and Fecova, K. (2006): Update on the mineral deposit potential of the Nootka Sound region (NTS 092E), west coast of Vancouver Island, British Columbia; *in* Geological Fieldwork 2005, BC Ministry of Energy, Mines and Petroleum Resources, Paper 2006-1 and Geoscience BC, Report 2006-1, p. 323–330.
- Marshall, D., Street, E., Ullrich, T., Xue, G., Close, S. and Fecova, K. (2006): Geology and mineral potential update for the Muchalat-Hesquiat region, Vancouver Island; *in* Geological Fieldwork 2005, BC Ministry of Energy, Mines and Petroleum Resources, Paper 2006-1 and Geoscience BC, Report 2006-1, p. 355–360.
- Massey, N.W.D. (1991): The geology of the Port Alberni–Nanaimo Lakes area; BC Ministry of Energy Mines and Petroleum Resources, Geoscience Map 1991-1.
- Massey, N.W.D., McIntyre, D.E., Desjardins, P.J. and Cooney, R.T. (2005): Digital geology map of British Columbia; BC Ministry of Energy, Mines and Petroleum Resources, Open File 2005-2.
- Muller, J.E., Cameron, B.E.B and Northcote, K.E. (1981): Geology and mineral deposits of the Nootka Sound map-area, Vancouver Island, British Columbia; Geological Survey of Canada, Paper 80-16, 53 p.
- Prendergast, M.D. (2000): Layering and precious metals mineralization in the Rincón del Tigre Complex, eastern Bolivia; *Economic Geology*, v. 95, p. 113–130.
- Renne, P.R., Swisher, C.C., Deino, A.L., Karner, D.B., Owens, T.L. and De-Paolo, D.J. (1998): Intercalibration of standards, absolute ages and uncertainties in  $^{40}\text{Ar}/^{39}\text{Ar}$  dating; *Chemical Geology*, v. 145, p. 117–152.
- Sargent, H. (1941): Supplementary report on Bedwell River area, Vancouver Island, British Columbia; British Columbia Department of Mines, Bulletin 13.
- Specogna, L. and Specogna, E. (2003): Fly One and Two; BC Ministry of Energy, Mines and Petroleum Resources, Assessment Report 27 214, 26 p.
- Taylor, H.P. and Noble, J.A. (1969): Origin of magnetite in the zoned ultramafic complexes of southeastern Alaska; *Economic Geology Monographs*, v. 4, p. 209–230.
- Yorath, C.J., Sutherland Brown, A. and Massey, N.W.D. (1999): LITHOPROBE, southern Vancouver Island, British Columbia; Geological Survey of Canada, Bulletin 498, 145 p.